Towards a Physics-Based Understanding of the L-H Transition Power Threshold*

L. Schmitz,[1] Z. Yan,[2] T.L. Rhodes,[1] P. Gohil,[3] G.R. McKee,[2] L. Zeng,[1] B. Grierson,[4] L. Bardoczi,[3] D. Eldon,[3] C.C. Petty[3]

[1]*University of California-Los Angeles, Los Angeles, CA 90095-7799, USA*
[2]*University of Wisconsin-Madison, Madison, WI 53706, USA*
[3]*General Atomics, PO Box 85608, San Diego, CA 92186-5608, USA*
[4]*Princeton Plasma Physics Laboratory, Princeton, NJ 08543-0451, USA*

Recent work at DIII-D has revealed important differences in L-H transition trigger dynamics between deuterium, helium and hydrogen plasmas. It is well established that the L-H transition power threshold in hydrogen plasmas is substantially higher, by as much as 70-150%, compared to deuterium (and helium) plasmas in DIII-D and in other tokamaks [1-4]. We test here our hypothesis that the ***E×B*** flow just inside the last closed flux surface (LCFS) is driven less effectively in hydrogen plasmas, therefore requiring higher power to trigger the L-H transition. We demonstrate that the toroidal flow correlation in hydrogen plasmas is substantially lower than in deuterium (and helium) plasmas. We also find that for similar plasma parameters the Reynolds force is lower in hydrogen, and the poloidal flow damping rate is higher. The Reynolds stress gradient is substantially larger than the torque associated with the bulk ion viscosity and ion orbit loss in deuterium and helium, but not in hydrogen. The ultimate goal of this work is to link differences in the microscopic turbulence-flow interaction to the resulting macroscopic isotope scaling, in order to advance a physics-based model of the L-H transition power threshold. The observed differences are qualitatively consistent with the observed higher power threshold in hydrogen.

The experiments were carried out in lower single

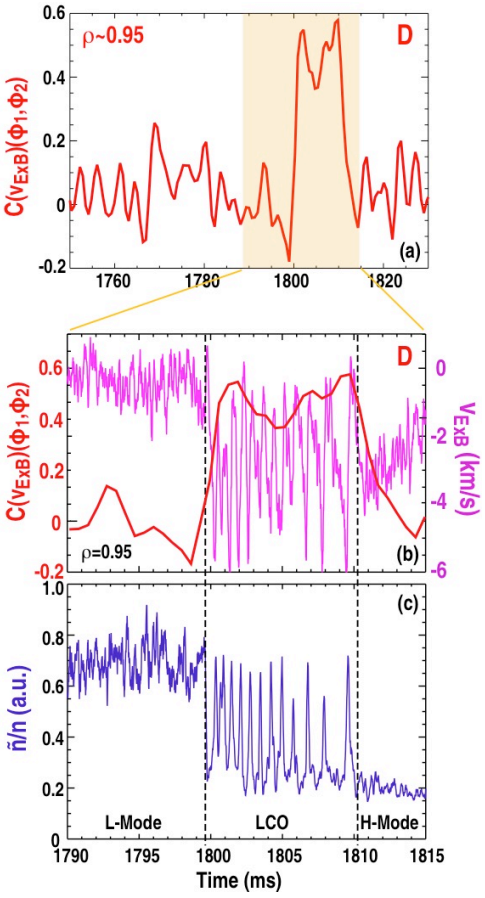

*Fig.1: (a) Cross-correlation coefficient of the **E×B** velocities measured in a D plasma at the same minor radius at two different toroidal positions (ϕ=60° and ϕ=240°), with the same poloidal launch angle, in ITER-similar plasmas (near the L-H threshold power of ~1.65 MW); (b) evolution of **E×B** velocity near the bottom of the E_r shear layer across the L-mode-LCO-H-mode transition; enlarged view of toroidal flow correlation; (c) evolution of density fluctuation level ($0.4 \le k_\perp \rho_s \le 0.7$).*

null plasma in the ITER-similar shape (ISS). Balanced torque injection (H, D) or low-torque co-injection (He) has been used at line-averaged densities of 2.6-3x10^{19} m^{-3}, and safety factor q_{95}~4.7-5.1, in the density range where a minimum in the L-H transition power threshold is observed [1,2]. The plasmas investigated here are characterized by a phase of limit cycle oscillations (LCO [5-7]) preceding the transition to H-mode. Plasmas with LCO allow detailed analysis of the changes in turbulence and plasma flows before significant changes in the edge pressure gradient occur (typically 1-10 ms after start of LCO).

Two different Doppler Backscattering diagnostic channels with identical frequency but different toroidal launch positions (ϕ_1=60º and ϕ_2=240º on the DIII-D midplane) are used for this measurement. Figure 1(a) shows the time evolution of the cross correlation coefficient (at zero time delay) between the $\boldsymbol{E}\times\boldsymbol{B}$ velocity measured at ρ=0.95 at the two different toroidal positions in a deuterium plasma in ISS shape (ITER-similar shape). No significant flow correlation is observed in L-mode prior to the L-mode-LCO transition. The flow correlation appears to decrease at later times near the LCO- to H-mode transition. This apparent loss of correlation for t >1812 ms is a measurement artifact due to the DBS probing radius moving out into the scrape-off layer once the pressure gradient responds and the H-mode pedestal begins to form. The probing radius after this time is at the outer edge of the shear layer where toroidal flow correlation is lower. An expanded view of the $\boldsymbol{E}\times\boldsymbol{B}$ velocity and the correlation coefficient [Fig. 1(b)] shows that the increase of the correlation coefficient slightly precedes, but basically occurs concomitantly with the development of oscillations in the $\boldsymbol{E}\times\boldsymbol{B}$ velocity at the transition to LCO. The maximum flow correlation coefficient is C~0.5-0.6.

Figure 2 shows the toroidal flow cross-correlation coefficient, determined from two DBS channels with identical frequency but a toroidal displacement of 180º, of the measured $\boldsymbol{E}\times\boldsymbol{B}$ flow during LCO, as probed in deuterium and hydrogen plasmas at the same density. $C[v_{ExB}(60º, 240º)]$ is substantially larger in D compared to H. No toroidal propagation delay is observed, indicating that the flow layer is forming in an axisymmetric fashion. Decreasing toroidal flow correlation has also been observed in TEXTOR Ohmic plasmas when the hydrogen- to deuterium fraction was increased [8].

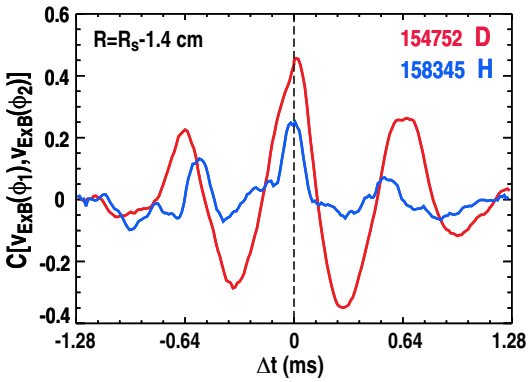

Fig. 2: Toroidal cross-correlation coefficient of $\boldsymbol{E}\times\boldsymbol{B}$ flow in D and H, at the indicated radius (ϕ_1=60º; ϕ_2=240º).

It is important to realize that the measured toroidal correlation implies toroidal as well as poloidal symmetry; following a fieldline, the rotational transform yields a difference in poloidal angle of ~35-40º between the two toroidally displaced outboard midplane DBS probing locations. As expected, there is no measurable toroidal correlation between the measured backscattered signal intensity (proportional to the density fluctuation power) as the

poloidal correlation length (~2-4 cm) is much smaller than the poloidal displacement between fieldlines intersecting both probing locations.

The time history of the ***E×B*** flow, turbulence level, and toroidal cross correlation in a hydrogen plasma, at very similar density density ($<n_e>$=2.6-2.7x10^{19}m^{-3}), is shown in Figure 3. The toroidal flow correlation increases again concomitantly with the first transient in the edge ***E×B*** flow. However in hydrogen $C \leq 0.25$, and the flow develops over a 2-3 ms time span, much slower than in D and He (He data not shown here). Less efficient flow drive in hydrogen is consistent with an increased power threshold, found to be more than two times higher compared to deuterium in the ISS shape in the intermediate density range considered here.

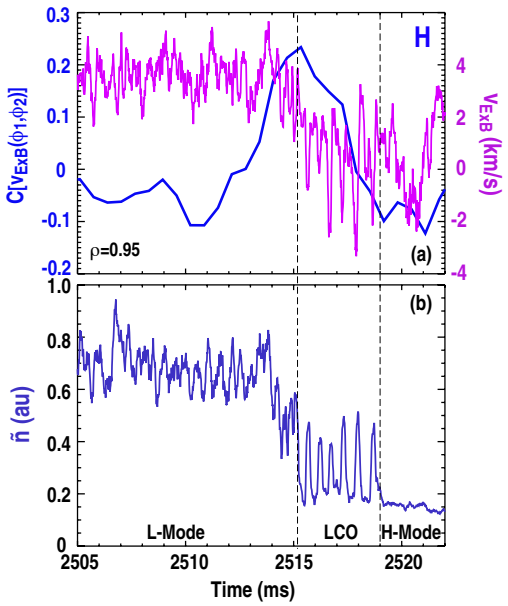

*Fig.3: (a) Toroidal cross-correlation coefficient C of the **E×B** velocity measured in hydrogen plasma at the same minor radius (toroidal angles ϕ=60° and ϕ=240°) (ISS plasma; L-H threshold power ~4.5 MW); evolution of **E×B** velocity and C near the bottom of the E_r shear layer; (b) evolution of density fluctuation level (measured for a poloidal wavenumber range $0.5 \leq k_\theta \rho_s \leq 0.9$.*

The non-ambipolar fluxes that establish the edge electric field layer can arise due to the turbulence-induced Reynolds stress and due to neoclassical contributions such as the bulk ion viscosity and the thermal ion orbit loss. Other contributions related to radial propagation of turbulent structures, and/or due to ion-neutral drag may also play a role under certain conditions [9,10] but are not considered here. Poloidal flow acceleration results from the $\boldsymbol{j \times B}$ force contributions due to these different terms. The poloidal flow damping rate in the edge layer is largest in hydrogen, as shown in Figure 4. The edge layer in D- and H-plasmas is in the plateau regime, with the poloidal flow damping rate $\nu_{i\theta}$ given by $\nu_{i\theta} = \nu_{tr}\varepsilon^{1/2}$, where ν_{tr} is the ion transit frequency. The helium edge plasma is in the Pfirsch-Schlueter regime with the damping rate given by ν_{tr}^2 / ν_{ii}, which is numerically smaller than the damping rates in D and H near the LCFS. Table I shows a comparison of correlation properties, and the contributions from the turbulent Reynolds stress (extracted from BES velocimetry [11]) for the outer shear layer, about 1 cm inside the last closed flux surface (LCFS) where the ***E×B*** shearing rate is highest. Similar values have been obtained for D-plasmas from reciprocating probe data [12,13]. The forces due to bulk viscosity and

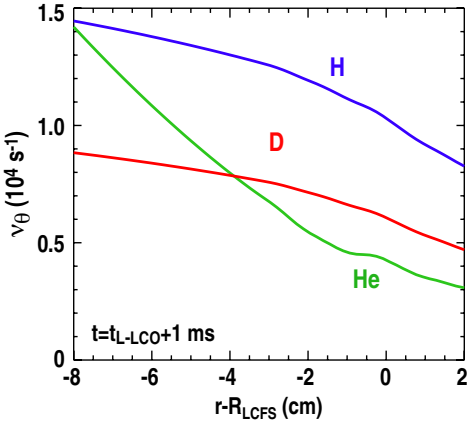

Fig.4: Poloidal flow damping rate in D, H, and He plasmas.

thermal orbit loss are estimated here based on simplified models discussed in [9,10]. The measured radial turbulence correlation length (shown here for a measured poloidal wavenumber range of $0.5 \le k_\theta \rho_s \le 0.9$) and the toroidal flow correlation length $L_{\phi E\times B}$ in the LCO phase are fairly similar in D and He (where P_{th} ~ 1.8 MW), but $L_{\phi E\times B}$ is much shorter in hydrogen plasmas. H-plasmas are concomitantly found to exhibit lower Reynolds stress [11], higher poloidal flow damping, and reduced toroidal correlation of the self-organized $\boldsymbol{E\times B}$ flow layer established in the plasma edge across the L-H transition. In addition, the Reynolds force acceleration is smaller than the (competing) acceleration terms due to viscous stress and thermal orbit loss in H, while the Reynolds force is substantially larger than these forces in D and He.

	$\tilde{n}/n$ (au)	L-H Trans. Time	L_r (cm)	$L_{\phi ExB}$ (cm)	ν_i*	$\nu_{i\theta}$ ($10^3 s^{-1}$)	F_{visc}/M_i ($10^9 m/s^2$)	F_{OL}/M_i ($10^9 m/s^2$)	F_{Rev}/M_i ($10^9 m/s^2$)
D	0.11	< 0.3 ms	0.6	1020	2.2	7	-1.4	0.9	-2.8
He	0.13	< 0.12ms	0.7	1414	9.1	4	-0.95	1.05	-4.5
H	0.07	1.6 ms	1.2	475	1.8	12	- 0.8	1.4	-0.63

Table I: Comparison of density fluctuation level, L-H transition time to establish enhanced negative E_r; radial turbulence correlation length, toroidal flow correlation length, normalized ion collisionality and poloidal flow damping rate, and acceleration due to bulk ion viscosity, thermal ion orbit loss, and Reynolds stress

The lower toroidal $\boldsymbol{E\times B}$ flow correlation across the L-H transition in hydrogen plasmas compared to D [Fig.1] and He indicates less effective production of the large-scale axisymmetric flow that triggers the L-H transition. All effects described here may contribute to, or explain the higher L-H transition threshold power required in hydrogen. More detailed studies are needed however to quantify the different force components in table I at both high and very low density/collisionality and systematically map their effect on the power threshold scaling.

*This material is based upon work supported by the U.S. Department of Energy, Office of Science, Office of Fusion Energy Sciences, using the DIII-D National Fusion Facility, a DOE Office of Science user facility, under Awards DE-FC02-04ER54698, DE-FG03-01ER54615, DE-AC02-09CH11466, DE-FG02-08ER54999, DIII-D data shown in this paper can be obtained in digital format by following the links at https://fusion.gat.com/global/D3D_DMP.

[1] P. Gohil, et al., Nucl. Fusion **51**,103020 (2011).
[2] G.R. McKee et al., Nucl. Fusion **49**, 115016 (2009).
[3] E. Righi, D.V. Bartlett, J.P. Christiansen, et al., Nucl. Fusion **39**, 309 (1999).
[4] F. Ryter, S.K. Rathgeber, L. Barrera Orte, M. Bernert, et al., Nucl. Fusion **53** 113003 (2013).
[5] L. Schmitz, L. Zeng, T.L. Rhodes, et al., Phys. Rev. Lett. **108**, 155002-5 (2012).
[6] K. Miki, P.H. Diamond, et al., Phys. Plasmas **19** 092306 (2012).
[7] L. Schmitz, et al., Nucl. Fusion **57**, 025003 (2017).
[8] Y. Xu, C. Hidalgo, I. Shesterikov, A. Kraemer-Flecken, et al., Phys. Rev. Lett. **110**, 265005 (2013).
[9] K. Itoh, Plasma Phys. Control. Fusion 36 A307-A318 (1994).
[10] J. Cornelis, R. Sporken, G. Van Oost, R.R. Weynants, Nucl. Fusion **34**, 171 (1994).
[11] Z. Yan, et al., 26th IAEA FEC conference, Oct 17-22, 2016, Kyoto, Japan, paper EX/5-1[12]
[12] G.R. Tynan, M. Xu, P.H. Diamond, J.A. Boedo, et al., Nucl. Fusion **53** 073053 (2013),
[13] J.A. Boedo, Prceedings of the 39th EPS conference on Plasma Physics, Stockholm, 2012, ocs.ciemat.es/epsicpp2012pap/pdf/P5.035.pdf.